

# Topological Phononics and Phonon Diode

Yizhou Liu<sup>1,2,3</sup>, Yong Xu<sup>1,2,3</sup>,\* Shou-Cheng Zhang<sup>4,5</sup>, and Wenhui Duan<sup>1,2,5†</sup>

<sup>1</sup>*State Key Laboratory of Low Dimensional Quantum Physics,  
Department of Physics, Tsinghua University,  
Beijing 100084, People's Republic of China*

<sup>2</sup>*Collaborative Innovation Center of Quantum Matter,  
Beijing 100084, People's Republic of China*

<sup>3</sup>*RIKEN Center for Emergent Matter Science (CEMS), Wako, Saitama 351-0198, Japan*

<sup>4</sup>*Department of Physics, McCullough Building,  
Stanford University, Stanford, California 94305-4045, USA*

<sup>5</sup>*Institute for Advanced Study, Tsinghua University,  
Beijing 100084, People's Republic of China*

## Abstract

Generalizing the concept of topology from electrons to phonons could bring in an intriguing emerging field of “topological phononics”. For this purpose we propose a Schrödinger-like equation of phonons where topology-related quantities, time reversal symmetry (TRS) and its breaking can be naturally introduced. A Haldane model of phonons for a two-dimensional honeycomb lattice is then developed to describe the interplay of symmetry and quantum (anomalous) Hall-like phonon states. The nontrivial topological phase supports one-way gapless edge states within the bulk gap, which can conduct phonons without dissipation. Moreover, breaking inversion symmetry and TRS simultaneously is suggested to open a route for valley phononics and phonon diode. The findings could help design unprecedented new phononic devices.

PACS numbers: 63.20.D-, 66.70.-f, 73.43.-f

The concept of topology has considerably revolutionized research of electronics since the discovery of topological insulators [1–3]. Novel quantum degrees of freedom like the Berry phase and topological order are utilized to control electrons, leading to an emerging field of “topological electronics” that is useful for low-power electronics, thermoelectrics, topological quantum computation, etc. [4–7]. On the other hand, the fast-growing field of phononics has attracted intensive research interest [8], but new ideas and devices are demanded to manipulate phonons efficiently. The marriage of topology and phononics may bring in a new paradigm phononics—“topological phononics”, which could find applications in heat dissipation, thermoelectrics, thermal insulation, phononic devices and so on.

Time reversal symmetry (TRS) plays an essential role in topological states. For electrons, integrating the Berry curvature over the Brillouin zone defines a topological invariant called the Chern number. Since the Berry curvature is odd under time reversal, the Chern number can be nonzero only when TRS is broken, which gives nontrivial topological states including the quantum Hall and quantum anomalous Hall states [9–12]. However, for phonons, very little is known about the influence of TRS breaking [13–16], and the interplay of symmetry and topology has been rarely studied, despite recent progress in integer Chern number states [16–19]. Theoretically, the typical treatment of phonons by dynamic matrix would fail if TRS is broken. Furthermore, how to generalize topological concepts from electrons to phonons remains unclear. A general theoretical framework of phonons is required to be developed for studying topological phononics and the effects of TRS breaking.

In addition, TRS breaking is favored for a key component of phononics—phonon diode, which conducts phonons in one direction but blocks phonons in the opposite direction. A general theorem tells that the nonreciprocal (or diode) effect would be zero in linear lossless systems with TRS for waves of any nature [20]. Thus one may design phonon diode based on nonlinearity or TRS breaking. Recent research mostly focuses on nonlinear systems [21, 22], but very little has been tried to break TRS, although the later method has been demonstrated to be successful elsewhere, for instance, in Faraday isolator of optics. Despite intensive effort, an ideal phonon diode with 100% efficiency has not yet been demonstrated [20].

In this Letter, we propose a Schrödinger-like equation of phonons in the extended coordinate-velocity space, which enables studying the influence of TRS breaking and generalizing the concept of topology from electrons to phonons. In an example study of a two-dimensional honeycomb lattice, we find a Haldane model of phonons that describes the interplay of symmetry and quantum

(anomalous) Hall-like phonon states. The novel topological phonon phase supports one-way gapless edge states within the bulk gap, which are immune to disorders and useful for designing low-dissipation phononic devices. Moreover, we suggest breaking inversion symmetry and TRS simultaneously to create valley-polarized phonon current and efficient phonon diode. A model of ideal phonon diode with 100% efficiency is proposed based on the one-way edge states in multi-terminal transport systems. Our findings shed new light on the development of topological phononics and phonon diode.

A typical Lagrangian of a crystal lattice in the harmonic approximation is written as

$$L_0 = \frac{1}{2}\dot{u}_i\dot{u}_i - \frac{1}{2}D_{ij}u_iu_j, \quad (1)$$

where  $u_i = \sqrt{m_i}x_i$ ,  $m_i$  is the atomic mass and  $x_i$  is the displacement for the  $i$ th degree of freedom, the mass-weighted force constant  $D_{ij} = \frac{\partial^2 V}{\partial u_i \partial u_j}|_{\mathbf{u}=0}$ ,  $V$  is the potential energy,  $i, j = 1, 2, \dots, dN$  for a  $d$ -dimensional system with  $N$  atoms. Einstein summation convention is used. The equation of motion of lattice vibration is  $\ddot{\mathbf{u}} = -D\mathbf{u}$ , whose Fourier transformation gives  $D_{\mathbf{k}}\mathbf{u}_{\mathbf{k}} = \omega_{\mathbf{k}}^2\mathbf{u}_{\mathbf{k}}$ . The eigenvalue problem of dynamic matrix  $D_{\mathbf{k}}$  determines the band dispersion  $\omega_{\mathbf{k}}$  and wavefunction  $\mathbf{u}_{\mathbf{k}}$  of phonons. This is a textbook result, for which TRS is implicitly assumed.

The only possible TRS-breaking term that is physically allowed in a harmonic Lagrangian has the form

$$L' = \eta_{ij}\dot{u}_i u_j, \quad (2)$$

where the coefficient matrix  $\eta$  is real and antisymmetric, as we proved in the Supplementary Material (SM) [23].

It is well known that TRS gets broken with an external magnetic field. Unlike electrons, neutral phonons do not couple with magnetic field directly. Indirect coupling, however, is possible in ionic lattices, where the Lorentz force on charged ions is nonzero [13, 16]. It is also possible in paramagnetic lattices by the Raman spin-lattice interaction [15, 16], which is used to explain the phonon Hall effect observed experimentally [14]. In addition to magnetic field  $\mathbf{B}$ , TRS can also be broken by applying a Coriolis field  $\mathbf{\Omega}$  through a rotating frame [18] or gyroscopic coupling [19]. The two kinds of fields are equivalent, since the Coriolis force  $2m\mathbf{v} \times \mathbf{\Omega}$  (mass  $m$  and velocity  $\mathbf{v}$ ) has the similar form as the Lorentz force  $q\mathbf{v} \times \mathbf{B}$  (charge  $q$ ). The Lagrangian of  $\mathbf{\Omega}$  is described by

Eq. (2), for which the submatrix  $\hat{\eta}_{\mu\nu}$  of  $\eta$  between atoms  $\mu$  and  $\nu$  is

$$\hat{\eta}_{\mu\nu} = \delta_{\mu\nu} \begin{pmatrix} 0 & -\Omega_z & \Omega_y \\ \Omega_z & 0 & -\Omega_x \\ -\Omega_y & \Omega_x & 0 \end{pmatrix}, \quad (3)$$

where  $\delta_{\mu\nu}$  is the Kronecker delta function. The Lagrangian of  $\mathbf{B}$  is obtained correspondingly by replacing  $\mathbf{\Omega}$  with  $q\mathbf{B}/2m$ .

After including the TRS-breaking term  $L'$ , the equation of motion of lattice vibration becomes  $\ddot{\mathbf{u}} = -D\mathbf{u} - 2\eta\dot{\mathbf{u}}$ . Its Fourier transformation changes into  $D_{\mathbf{k}}\mathbf{u}_{\mathbf{k}} - 2i\omega_{\mathbf{k}}\eta_{\mathbf{k}}\mathbf{u}_{\mathbf{k}} = \omega_{\mathbf{k}}^2\mathbf{u}_{\mathbf{k}}$ . Noticeably, this equation is no longer an eigenvalue problem (since  $\eta_{\mathbf{k}}$  is a matrix), and the solution  $\mathbf{u}_{\mathbf{k}}$  is not an eigenmode anymore. The traditional way of studying phonons by solving eigen equations in the coordinate space gets failed. Some fundamental problems arise: How to properly define the wavefunction, Berry phase and topological invariant for phonons? How to describe the effects of TRS breaking in phonon transport? These issues are essential to explore emerging physics of phonons with broken TRS, like topological states and nonreciprocal transport.

Let us borrow ideas from electrons. If we could find a Schrödinger-like equation for phonons, all the above problems would be naturally solved. However, this is not a straightforward task, because the Schrödinger equation of electrons is first order in time and can have positive and negative energies, whereas the Lagrangian equation of phonons is second order in time and has non-negative frequencies only [24]. Inspiration is obtained from Dirac, who discovered the famous Dirac equation by creatively taking a “square root” of the Klein-Gordan equation. We thus tried to find a “square root” for the problem of lattice vibration.

Intriguingly, for phonons the “square root” of Lagrangian (or Newtonian) mechanics actually is Hamiltonian mechanics. Based on Hamiltonian mechanics, we can derive a *Schrödinger-like equation of phonons*:  $H_{\mathbf{k}}\psi_{\mathbf{k}} = \omega_{\mathbf{k}}\psi_{\mathbf{k}}$ , where

$$H_{\mathbf{k}} = \begin{pmatrix} 0 & iD_{\mathbf{k}}^{1/2} \\ -iD_{\mathbf{k}}^{1/2} & -2i\eta_{\mathbf{k}} \end{pmatrix}, \quad \psi_{\mathbf{k}} = \begin{pmatrix} D_{\mathbf{k}}^{1/2}\mathbf{u}_{\mathbf{k}} \\ \dot{\mathbf{u}}_{\mathbf{k}} \end{pmatrix}. \quad (4)$$

This is a key result of the present work. The derivation details are included in the SM [23]. Here  $D_{\mathbf{k}}$  is positive-semidefinite as required by the structural stability, and its square root  $D_{\mathbf{k}}^{1/2}$  is thus Hermitian, which together with the anti-Hermitian  $\eta_{\mathbf{k}}$  gives a Hermitian Hamiltonian  $H_{\mathbf{k}}$ . The equation has some important features:

(i) The phonon wavefunction  $\psi_{\mathbf{k}}$  is defined in the extended coordinate-velocity space, including two subspaces  $\psi_{\mathbf{k}}^1 = D_{\mathbf{k}}^{1/2} \mathbf{u}_{\mathbf{k}}$  and  $\psi_{\mathbf{k}}^2 = \dot{\mathbf{u}}_{\mathbf{k}}$ . For systems with TRS,  $\eta_{\mathbf{k}} = 0$ , leading to zero coupling between the two subspaces. Thus using either subspace is enough to describe phonons. The situation is similar for electrons. While the two-component spinor wavefunction is required in general, only the one-component wavefunction is necessary for describing spin-degenerate systems.

(ii) The phonon Hamiltonian has  $2dN$  eigenvalues, but the system only has  $dN$  degrees of freedom. The discrepancy is explained by a ‘‘particle-hole’’ symmetry,  $\{H, K\} = 0$  ( $K$  is the complex conjugate operator), which guarantees  $(\omega_{\mathbf{k}}, \psi_{\mathbf{k}})$  and  $(-\omega_{-\mathbf{k}}, \psi_{\mathbf{k}}^*)$  appear in pairs.

(iii) Based on the Schrödinger-like equation, all topology-related quantities of phonons can be defined similar as for electrons. For the  $n$ th band,  $\psi_{n\mathbf{k}}$  is the phonon wavefunction, the Berry connection  $\mathbf{A}_{n\mathbf{k}} = -i\psi_{n\mathbf{k}}^\dagger \nabla_{\mathbf{k}} \psi_{n\mathbf{k}}$ , the Berry curvature  $\mathbf{B}_{n\mathbf{k}} = \nabla_{\mathbf{k}} \times \mathbf{A}_{n\mathbf{k}}$ , and the Chern number  $C_n = \frac{1}{2\pi} \iint_{BZ} d^2\mathbf{k} B_{z,n\mathbf{k}}$ . The total Chern number  $C$  is the summation over all the Chern numbers of bands below a specified band gap.

(iv) Under inversion symmetry,  $\omega_{n\mathbf{k}} = \omega_{n,-\mathbf{k}}$  and  $\mathbf{B}_{n\mathbf{k}} = \mathbf{B}_{n,-\mathbf{k}}$ . Under TRS,  $\omega_{n\mathbf{k}} = \omega_{n,-\mathbf{k}}$ ,  $\mathbf{B}_{n\mathbf{k}} = -\mathbf{B}_{n,-\mathbf{k}}$  and  $C \equiv 0$ .

For phonon transport, the nonequilibrium Green’s function (NEGF) method has been widely used to study the problem quantum mechanically, which is able to describe linear phonon systems accurately and provide a systematic way to treat many-body interactions [25–27]. However, the existing NEGF method works only for phonons with TRS. The approach has to be generalized to describe phonons with broken TRS. Here based on the Schrödinger-like equation of phonons, we derived a generalized formalism of the NEGF method for exploring the effects of TRS breaking in phonon transport. The method details are described in the SM [23].

Next we apply the developed theory to study a model system of a two-dimensional honeycomb lattice [Fig.1(a)] with in-plane vibrations. Interatomic couplings with nearest- and next-nearest neighbors are included and described by springs of force constants  $k_1$  and  $k_2$ , respectively. Atomic masses of the two sublattices  $m_A = m(1 - \delta)$  and  $m_B = m(1 + \delta)$  are tuned by  $\delta$  that breaks the inversion symmetry. A Coriolis field  $\boldsymbol{\Omega}$  of out-of-plane angular velocity  $\Omega_z$  (or a magnetic field  $\mathbf{B}$ ) is introduced to break TRS [Fig.1(a)]. Let us begin with  $\delta = 0$  and  $\Omega_z = 0$ . As presented in Fig.1(b), both acoustic and optical bands are doubly degenerate at the  $\Gamma$  point and get split away from  $\Gamma$ . The longitudinal acoustic (LA) and longitudinal optical (LO) bands form Dirac-like linear dispersions at the  $K$  ( $K'$ ) point. The Dirac point is located at  $\omega_D = \sqrt{(3k_1 + 9k_2)/2m}$ , where the group velocity is  $v_D = 3k_1 a / 8m\omega_D$  ( $a$  is the nearest neighbor distance).  $k_1 = 1$ ,  $k_2 = 0.05$ ,  $m = 1$

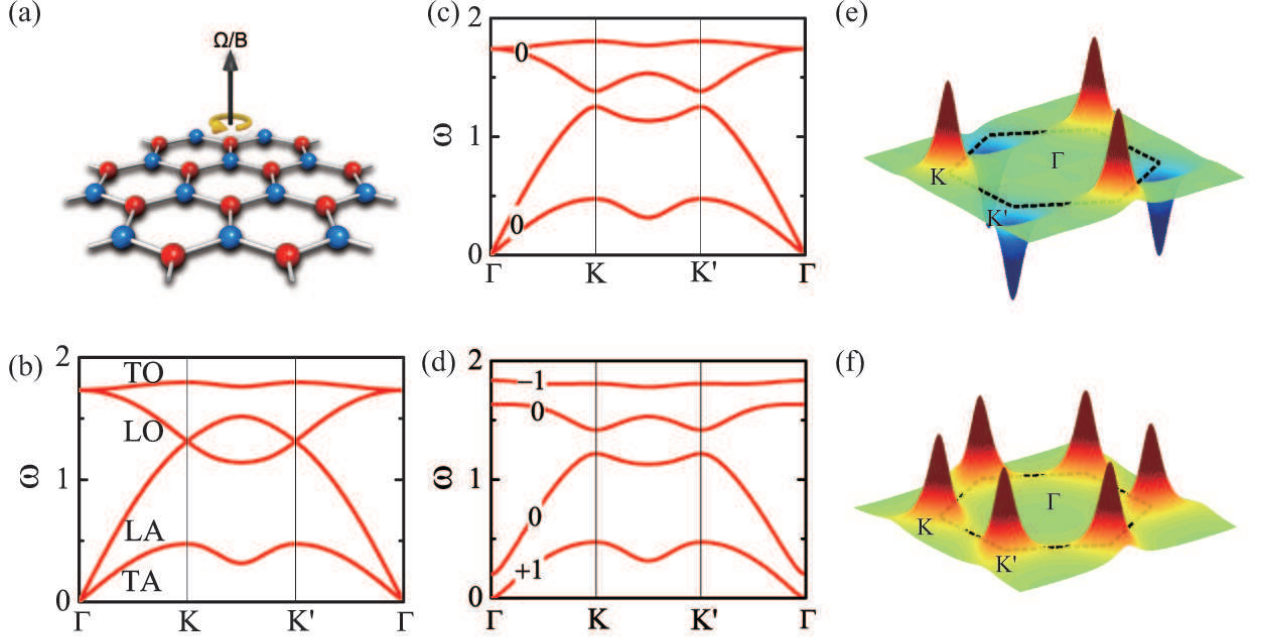


FIG. 1: (a) A two-dimensional honeycomb lattice with nearest- and next-nearest-neighbor couplings. The two sublattices are colored blue and red. TRS is broken by a Coriolis field  $\Omega$  or a magnetic field  $\mathbf{B}$ . (b) The phonon dispersion with preserved inversion symmetry and TRS ( $m_I = m_T = 0$ ), where Dirac-like linear dispersions exist at the  $K$  and  $K'$  points. “TA”, “LA”, “TO” and “LO” denote transverse acoustic, longitude acoustic, transverse optical, longitude optical modes, respectively. (c,d) The Phonon dispersions with broken inversion symmetry (c:  $m_I = 0.1$ ) and broken TRS (d:  $m_T = 0.1$ ), where a band gap is opened at the Dirac point. Chern numbers of separated bands are labelled. (e,f) Distribution of the Berry curvature in the Brillouine zone for the two lowest bands of dispersions in (c) and (d), respectively.

and  $a = 1$  were selected without loss of generality.

To study the interplay of symmetry and topology, we derive an effective Hamiltonian of phonons around the Dirac point based on symmetry analysis (see details in the SM [23]):

$$H_0(\mathbf{k}) = v_D (k_y \tau_z \sigma_x - k_x \sigma_y), \quad (5)$$

where  $\mathbf{k}$  is referenced to  $K$  ( $K'$ ) and  $\omega_{\mathbf{k}}$  to  $\omega_D$ .  $\sigma$  and  $\tau$  are the Pauli matrices with  $\sigma_z = \pm 1$  and  $\tau_z = \pm 1$  referring to  $A(B)$  sublattice and valley index  $K$  ( $K'$ ), respectively. This Hamiltonian describes the linear gapless phonon dispersions at  $K$  ( $K'$ ) with  $\omega_{\mathbf{k}} = \pm v_D |\mathbf{k}|$ . The degeneracy of the Dirac point is protected by inversion symmetry and TRS. If terms proportional to  $\sigma_z$  and  $\sigma_z \tau_z$

are added into the Hamiltonian, a band gap could be opened at the Dirac point.  $\sigma_z$  is odd under parity that exchanges the  $A$  and  $B$  sublattices.  $\tau_z$  is odd under both parity and time reversal that exchanges the  $K$  and  $K'$  valleys. Thus the  $\sigma_z$  term breaks inversion symmetry and the  $\sigma_z\tau_z$  term breaks TRS.

When  $\delta \neq 0$ , an inversion symmetry-breaking mass term

$$H'_I = m_I \sigma_z \quad (6)$$

is added into the effective Hamiltonian with  $m_I = \frac{\delta}{2} \omega_D$  [23]. This results in a band gap of  $2m_I$  at the Dirac point with  $\omega_{\mathbf{k}} = \pm \sqrt{(v_D |\mathbf{k}|)^2 + m_I^2}$ , as shown in Fig.1(c).

When  $\Omega_z \neq 0$ , a TRS-breaking mass term

$$H'_T = m_T \sigma_z \tau_z \quad (7)$$

is added into the effective Hamiltonian with  $m_T = \Omega_z$  [23]. Noticeably, this is reminiscent of the well-known Haldane model [11], the first model for a quantum Hall effect without Landau levels (i.e. the quantum anomalous Hall effect). The Haldane model was originally proposed for spinless electrons. We for the first time find a *Haldane model of phonons*, which helps us understand the novel quantum (anomalous) Hall-like phonon states, as demonstrated below.

With broken TRS, a band gap of  $2m_T\tau_z$  is opened at the Dirac point with  $\omega_{\mathbf{k}} = \pm \sqrt{(v_D |\mathbf{k}|)^2 + (m_T \tau_z)^2}$  [see Fig.1(d)]. The band gap at the  $K$  and  $K'$  points has opposite signs ( $2m_T$  at  $K$  point and  $-2m_T$  at  $K'$ ), indicating an inverted band order. To smoothly transform into trivial insulators in the atomic limit, a band inversion must happen and the band gap must be closed at the critical transition point. In contrast, the band gap generated by  $H'_I$  has the same sign at the  $K$  and  $K'$  points, which can be adiabatically connected to trivial atomic insulators. Therefore, the Dirac gap (i.e., the band gap around the Dirac point) induced by  $H'_T$  and  $H'_I$  belong to two different topological classes. One is topologically nontrivial, while the other is not.

To verify the topological nature, we calculate the Berry curvature and Chern number for the Dirac gap. When  $m_I = m_T = 0$ , the Berry curvature  $B_{z,\mathbf{k}}$  is zero everywhere except at the degenerate Dirac points where it diverges. The Berry phase enclosing the Dirac point is  $\pi$  ( $-\pi$ ) at  $K$  ( $K'$ ). With a small nonzero mass term,  $B_{z,\mathbf{k}}$  displays finite peaks centered at  $K$  and  $K'$  and is nearly zero elsewhere [Fig. 1(e,f)]. The integration of each peak gives a Berry phase of  $\pm\pi$ . Berry phases of the two peaks cancel when breaking inversion symmetry, giving  $C = 0$ ; they add when breaking TRS, giving  $C = 1$ .

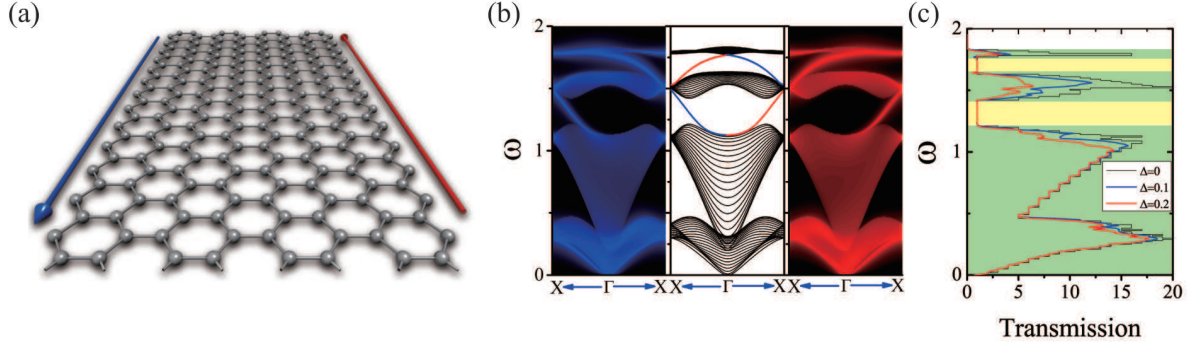


FIG. 2: (a) Schematic of a nanoribbon structure with one-way edge states. (b) The phonon dispersion (middle) and density of states projected onto the left and right edges (left and right) for a nanoribbon structure consisted of 20 zigzag chains with broken TRS ( $m_T = 0.1$ ). Large (small) density of states are colored blue/red (black). In the Dirac gap, backward-moving (blue) and forward-moving (red) edge states exist only on the left and right, respectively. (c) Phonon transmissions as a function of frequency for the nanoribbon with and without disorders. Disorders are introduced into the center part of a length of 20 unit cells by selecting atomic masses randomly within  $[1 - \Delta, 1 + \Delta]$ . Results of  $\Delta = 0, 0.1, 0.2$  are denoted by black, red and blue lines, respectively. The phonon transmission decreases gradually with increasing  $\Delta$ , except for the one-way edge states within the bulk gap (shaded yellow).

One prominent feature of the topological phonon phase with nonzero Chern number is the existence of gapless edge states that propagate in one direction. The one-way edge states are immune to disorders because no states are available for backscattering. To demonstrate this feature explicitly, we consider a nanoribbon structure [illustrated in Fig. 2(a)]. For  $m_T \neq 0$ , gapless edge states are clearly visualized within the Dirac gap, which are forward-moving along one edge and backward-moving along the other edge, as shown in the band structure and projected density of states [Fig. 2(b)]. We further performed NEGF transport calculations to explore disorder effects. As shown in Fig. 2(c), disorder scattering suppresses transmission of all phonon states except the one-way edge states. The edge-state transport is ballistic and unaffected by disorders due to its unidirectional nature.

In more general cases with nonzero  $m_I$  and  $m_T$ , the band gaps are  $2(m_I + m_T)$  and  $2(m_I - m_T)$  at the  $K$  and  $K'$  points, respectively. The competition between the two types of mass terms determines the band topology of the Dirac gap, as summarized in the phase diagram of Fig. 3(a). For  $|m_T| <$

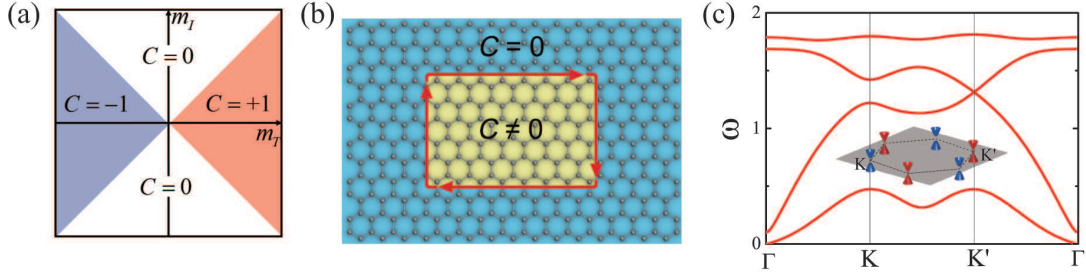


FIG. 3: (a) A phase diagram showing that the Chern number  $C$  of the Dirac gap is tuned by the two types of mass terms  $m_I$  and  $m_T$ . (b) Schematic of patterning one-way edge states (denoted by red lines) at the interface between regions of  $C = 0$  and  $C \neq 0$ . (c) The phonon dispersion of  $m_I = m_T = 0.05$ , in which one Dirac point at  $K'$  is preserved and the other one at  $K$  is gapped as illustrated in the inset. This is an example showing that the band degeneracy of the  $K$  and  $K'$  valleys is split by breaking inversion symmetry and TRS simultaneously.

$|m_I|$ , the band gap has the same sign between  $K$  and  $K'$  and  $C = 0$ ; for  $|m_T| > |m_I|$ , the Dirac gap has opposite signs between  $K$  and  $K'$  and  $C = 1$ . This phase diagram provides a guidance for designing topological phononics. As a potential application, the one-way edge states can be used as dissipationless conducting wires for phononic circuits. They can be patterned in a controlled way as illustrated in Fig. 3(b). For a given geometry, topological phase boundaries are designed with different  $m_I$  ( $m_{I1}$  and  $m_{I2}$ ) and a homogenous TRS-breaking field  $m_T$ . The one-way edge states exist at the boundary when  $|m_{I1}| < |m_T| < |m_{I2}|$  and disappear otherwise. To visualize the lattice dynamics, we performed molecular dynamics calculations and indeed observed that lattice vibrations of frequencies within the Dirac gap can transport unidirectionally along the patterned boundary. The calculation details and snapshots of a movie are included in the SM [23].

Furthermore, the valley degree of freedom can be greatly tuned by varying the two types of mass terms. Specifically, magnitudes of the Dirac gaps can be significantly different for the  $K$  and  $K'$  valleys, which is potentially useful for valley phononics. For instance, when  $m_I = m_T \neq 0$ , a novel phonon dispersion with a Dirac gap at the  $K$  valley and a gapless Dirac cone at the  $K'$  valley will appear [Fig. 3(c)]. A 100% valley-polarized phonon current could be realized when the input phonon frequency is selected within the Dirac gap of the  $K$  valley.

In the above discussion, we mainly focus on properties of the Dirac gap. Actually, the two-fold band degeneracies at the  $\Gamma$  point can be lifted by the Coriolis or magnetic field [Fig. 1(d)]. This

opens two additional band gaps at the  $\Gamma$  point. Both of them are topologically nontrivial ( $C = 1$ ) when  $m_T \neq 0$ , insensitive to the parameter  $m_I$ . The one-way edge states would appear between the split bands if a global band gap exists between them, which is the case for the gap between the 3rd and 4th bands [see Fig. 2(b)].

In the following we will discuss the role of TRS breaking in the context of phonon diode. For systems with TRS, the forward- and backward-moving states would always appear in pairs. Thus it is extremely challenging, if not impossible, to realize an ideal phonon diode that gives transmission of 100% in one direction and 0% in the opposite direction. The observed diode effect is very weak in experiments when TRS is preserved [22]. Naturally one may break TRS to disentangle the forward- and backward-moving states for improving the diode effect. The topological phonon states are promising for the purpose, because their unique one-way edge states intrinsically are perfect diode channels. However, only breaking TRS is not enough for generating diode effect, since the symmetry between  $\mathbf{k}$  and  $-\mathbf{k}$  states is ensured by TRS as well as inversion symmetry. It is thus necessary to break both symmetries simultaneously to create phonon diode in linear (or harmonic) systems.

To see diode effect explicitly, we considered a typical two-terminal transport system as shown in the inset of Fig. 4(a), broke its symmetries with nonzero  $\delta$  and  $\Omega_z$ , and simulated phonon transport by the NEGF method. Unfortunately, the calculated phonon transmission is always direction-independent, even though different parameters, defects or disorders were introduced. The result is straightforward for one-way edge states, whose diode effect gets cancelled by the two opposite edges [Fig. 4(a)]. However, the absence of diode effect in generic phonon states is not expected from the above symmetry argument.

The result can be understood as follows. Phonon transport through a linear system is described by a scattering matrix  $S$ . The matrix element  $S_{ij}$  characterizes the complex amplitude of an output in the  $j$ th terminal induced by an input of unity amplitude in the  $i$ th terminal.  $S$  is unitary as required by power conservation. If together with TRS that requires  $S^{-1} = S^*$  [20],  $S$  would be symmetric,  $S_{ij} = S_{ji}$ , giving zero diode effect.  $S$  is generally not symmetric when TRS is broken. However, for a two-terminal transport system, the unitary condition of  $|S_{12}|^2 + |S_{11}|^2 = |S_{21}|^2 + |S_{22}|^2 = 1$  enforces a direction-independent transmission  $|S_{12}|^2 = |S_{21}|^2$  even with broken TRS. Phonon diode effect appears only in multi-terminal transport systems (see below). Note that the conclusion applies only to a purely coherent system. Nonzero diode effect is possible for a two-terminal transport system if including the phase-breaking effect that can be simulated by

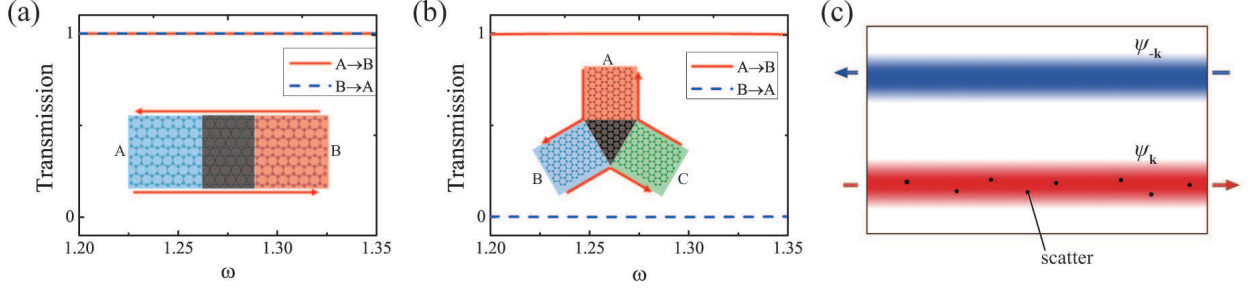


FIG. 4: (a,b) Phonon transmissions as a function of frequency from terminal A to B (red solid line) and from B to A (blue dashed line) for (a) two-terminal and (b) three-terminal transport systems (shown in the insets using red lines to denote one-way edge states) with  $m_I = 0, m_T = 0.1$ . Results are shown only for phonon frequencies within the Dirac gap. The former system gives zero diode effect. The latter acts as an ideal phonon diode with 100% efficiency. (c) A schematic diagram illustrating the concept of selective scattering for enhancing the diode effect. When TRS is broken, the real-space distribution of the forward-/backward-moving states ( $\psi_{\mathbf{k}}/\psi_{-\mathbf{k}}$ ) (denoted by red/blue colors) can be space separated. With such kind of feature, scatters (denoted by black dots) are placed onto the transport path of the forward-moving state only, selectively scattering the forward-moving channel.

attaching probe terminals in the scattering region [28, 29].

Then we study a three-terminal transport system as shown in the inset of Fig. 4(b). The one-way edge states can result in perfect diode effect between any two of the terminals. For instance, the edge states flow from terminal A to B without any scattering and the back flow from B to A is exactly zero (since an input from B all flows out through C). This physical picture is verified by the NEGF transport calculations (see the results in Fig. 4(b)). Therefore, an ideal phonon diode with 100% efficiency can be realized by one-way edge states in a multi-terminal setup. As far as we know, this is the first model of ideal phonon diode, which is useful for building efficient phononic devices.

For generic phonon states, the diode effect can be tuned based on the information of real-space distribution of phonon states (i.e.,  $\psi_{\mathbf{k},\mu}$ , the wave function projected onto the  $\mu$ -th atom). When TRS is broken, we generally have  $|\psi_{\mathbf{k},\mu}|^2 \neq |\psi_{-\mathbf{k},\mu}|^2$ . Then for some specific phonon modes, the forward- and backward-moving states ( $\psi_{\mathbf{k}}$  and  $\psi_{-\mathbf{k}}$ ) can be separated in real space as schematically shown in Fig. 4(c), which is confirmed by our calculations (data not shown). With such a space-

separated feature, it is possible to introduce defects/disorders mainly along the transport path of  $\psi_{\mathbf{k}}$ . As a result, the state  $\psi_{\mathbf{k}}$  will be scattered by the defects/disorders, whereas the opposite-moving state  $\psi_{-\mathbf{k}}$  is much less affected. This concept of selective scattering [illustrated in Fig. 4(c)] can be used to enhance diode effect, which will be explored in details in our future work. Our findings of topological phononics and phonon diode can be applied to control sound and heat, though the manipulation of heat conduction is relatively more challenging because all the thermally excited phonons are involved in the process.

Y.X. acknowledges support from the National Thousand-Young-Talents Program and Tsinghua University Initiative Scientific Research Program. Y.L. and W.D. acknowledge support from the Ministry of Science and Technology of China (2016YFA0301000) and the National Natural Science Foundation of China (11334006). S.C.Z is supported by the NSF under grant numbers DMR-1305677.

---

\* Electronic address: yongxu@mail.tsinghua.edu.cn

† Electronic address: dwh@phys.tsinghua.edu.cn

- [1] C. L. Kane and E. J. Mele, *Phys. Rev. Lett.* **95**, 226801 (2005).
- [2] B. A. Bernevig, T. L. Hughes, and S.-C. Zhang, *Science* **314**, 1757 (2006).
- [3] M. König, S. Wiedmann, C. Brüne, A. Roth, H. Buhmann, L. W. Molenkamp, X.-L. Qi, and S.-C. Zhang, *Science* **318**, 766 (2007).
- [4] X.-L. Qi and S.-C. Zhang, *Phys. Today* **63**, 33 (2010).
- [5] M. Z. Hasan and C. L. Kane, *Rev. Mod. Phys.* **82**, 3045 (2010).
- [6] X.-L. Qi and S.-C. Zhang, *Rev. Mod. Phys.* **83**, 1057 (2011).
- [7] Y. Xu, Z. Gan, and S.-C. Zhang, *Phys. Rev. Lett.* **112**, 226801 (2014).
- [8] M. Maldovan, *Nature* **503**, 209 (2013).
- [9] K. v. Klitzing, G. Dorda, and M. Pepper, *Phys. Rev. Lett.* **45**, 494 (1980).
- [10] D. J. Thouless, M. Kohmoto, M. P. Nightingale, and M. den Nijs, *Phys. Rev. Lett.* **49**, 405 (1982).
- [11] F. D. M. Haldane, *Phys. Rev. Lett.* **61**, 2015 (1988).
- [12] C.-Z. Chang, J. Zhang, X. Feng, J. Shen, Z. Zhang, M. Guo, K. Li, Y. Ou, P. Wei, L.-L. Wang, et al., *Science* **340**, 167 (2013).
- [13] A. Holz, *Il Nuovo Cimento B* **9**, 83 (1972).

- [14] C. Strohm, G. L. J. A. Rikken, and P. Wyder, *Phys. Rev. Lett.* **95**, 155901 (2005).
- [15] L. Sheng, D. N. Sheng, and C. S. Ting, *Phys. Rev. Lett.* **96**, 155901 (2006).
- [16] L. Zhang, J. Ren, J.-S. Wang, and B. Li, *Phys. Rev. Lett.* **105**, 225901 (2010).
- [17] E. Prodan and C. Prodan, *Phys. Rev. Lett.* **103**, 248101 (2009).
- [18] Y.-T. Wang, P.-G. Luan, and S. Zhang, *New J. Phys.* **17**, 073031 (2015).
- [19] P. Wang, L. Lu, and K. Bertoldi, *Phys. Rev. Lett.* **115**, 104302 (2015).
- [20] A. Maznev, A. Every, and O. Wright, *Wave Motion* **50**, 776 (2013).
- [21] B. Li, L. Wang, and G. Casati, *Phys. Rev. Lett.* **93**, 184301 (2004).
- [22] C. Chang, D. Okawa, A. Majumdar, and A. Zettl, *Science* **314**, 1121 (2006).
- [23] Supplementary Materials.
- [24] C. Kane and T. Lubensky, *Nature Phys.* **10**, 39 (2014).
- [25] Y. Xu, J.-S. Wang, W. Duan, B.-L. Gu, and B. Li, *Phys. Rev. B* **78**, 224303 (2008).
- [26] J.-S. Wang, J. Wang, and J. Lü, *Eur. Phys. J. B* **62**, 381 (2008).
- [27] Y. Xu, X. Chen, J.-S. Wang, B.-L. Gu, and W. Duan, *Phys. Rev. B* **81**, 195425 (2010).
- [28] M. Büttiker, *IBM J. Res. Dev.* **32**, 63 (1988).
- [29] S. Datta, *Electronic transport in mesoscopic systems* (Cambridge university press, 1997).